

Optical Hall conductivity of systems with gapped spectral nodes

Antonio Hill¹, Andreas Sinner¹ and Klaus Ziegler¹

Institut für Physik, Universität Augsburg,
Universitätsstraße 1, D-86159 Augsburg, Germany

Received: date / Revised version: date

Abstract. We calculate the optical Hall conductivity within the Kubo formalism for systems with gapped spectral nodes, where the latter have a power-law dispersion with exponent n . The optical conductivity is proportional to n and there is a characteristic logarithmic singularity as the frequency approaches the gap energy. The optical Hall conductivity is almost unaffected by thermal fluctuations and disorder for $n = 1$, whereas disorder has a stronger effect on transport properties if $n = 2$.

PACS. XX.XX.XX No PACS code given

1 Introduction

Transport properties of systems with two bands and spectral nodes are of great interest, as recent studies of graphene have indicated. A prototype of this material class is monolayer graphene (MLG) which is a monoatomic sheet of carbon atoms arranged in a honeycomb lattice with unique transport properties. This is a consequence of the two-dimensional nature of the material and due to the band structure which consists of two separate bands touching one another at isolated nodes. In the vicinity of these nodes quasiparticles exhibit a linear spectrum. The main difference between MLG and bilayer graphene (BLG) is that the low-energy excitations of the latter have a quadratic spectrum [1,2]. For the longitudinal conductivity this difference causes a factor of 2 for the DC conductivity [3, 4] and also for the optical conductivity [5]. Additionally, we found a logarithmic singularity in the optical Hall conductivity for MLG in an earlier work [6]. This leads to the question how a change of the low-energy spectrum around the nodes affects the quantum Hall properties and the singularity, e.g., for a few layers of graphene. For this purpose we generalize our model and assume that the spectrum in a small vicinity of the node is a power law with integer n ($n \geq 1$). We will call this spectral structure a node of order n .

An intriguing phenomenon in graphene is the quantum Hall effect (QHE) which was already observed in the first experiments on graphene [7]. It exhibits a rather unexpected anomalous behavior. In contrast to the QHE in a two-dimensional electron gas of a semiconductor, the Hall plateaux appear antisymmetrically around zero carrier density [1]. The existence of these plateaux is commonly explained by a nonzero Berry phase [1,7,8,9]. Additionally, the magnitude of the Hall conductivity of the first plateau is for BLG twice the corresponding value of

MLG [1]. Similar effects appear in the case of rhombohedral (ABC) stacked trilayer graphene where the first plateau is found to be three times higher than in MLG [10]. It is widely accepted that the QHE occurs in semimetals as a consequence of a gap opening and broken time reversal symmetry. Usually, this is achieved by applying a magnetic field perpendicular to the 2D plane, whereas the gap opening alone can be obtained by hydrogenation of MLG [11] or by a double gate in the case of BLG [2]. The optical Hall conductivity was calculated for graphene in a homogeneous magnetic field [12,13,14].

An alternative way for observing the QHE was suggested by Haldane, using a periodic magnetic flux on the honeycomb lattice [15]. Such a periodic flux can be generated by a spin texture, realized by spin doping of graphene [6]. The main effect of the periodic flux is that the mass terms in the two valleys can be tuned independently. Then the QHE appears when the mass signs in the two valleys are different because the Hall conductivity reads [6]

$$\sigma_{xy} = [\text{sgn}(m) - \text{sgn}(m')] \frac{e^2}{2h}. \quad (1)$$

A similar case is a 3D topological insulator whose surface is covered with magnetically ordered spins [16]. The spins break the time-reversal invariance and open a gap in the surface Dirac cones.

2 Model

In the following we calculate the Hall conductivity for low-energy quasiparticles in the vicinity of a node with a uniform gap and a power-law spectrum with integer exponent. Then the low-energy Hamiltonian, describing electrons in systems with spectral nodes with a uniform

gap $\Delta = 2m$, reads in Fourier representation as

$$H = \gamma \begin{pmatrix} \gamma m & (k_x - ik_y)^n \\ (k_x + ik_y)^n & -\gamma m \end{pmatrix}, \quad (2)$$

where $n = 1$ should be associated with MLG and $n = 2$ with BLG. For general order n the eigenvalues of the Hamiltonian are

$$E_l = (-1)^l E, \quad E = \gamma \sqrt{(\gamma m)^2 + k^{2n}}, \quad (3)$$

where $l = 0$ ($l = 1$) refer to the upper (lower) band, respectively. The band parameter γ is for example in MLG $\gamma = v_F$ [17] and in BLG $\gamma = v_F^2/\gamma_1$ [18], where v_F is the Fermi velocity and γ_1 is the interlayer coupling constant. To simplify the notation we drop indices for spin- and valley degeneracy and put γ equal to unity. The corresponding eigenvectors are

$$\psi_k^\pm(\mathbf{r}) = \sqrt{\frac{E \mp m}{2E}} \begin{pmatrix} (k_x - ik_y)^n \\ \pm E - m \end{pmatrix} \exp(i\mathbf{k} \cdot \mathbf{r}). \quad (4)$$

If the stacking order of the layers is of type ABC, n can be associated with the number of layers, and the effective low-energy Hamiltonian is given by Eq. (2) [19,20].

3 Optical Hall conductivity

The Hall conductivity can be calculated as the off-diagonal element of the Kubo conductivity tensor:

$$\sigma_{\mu\nu} = \lim_{\alpha \rightarrow 0} \frac{i}{\hbar} \int \sum_{l,l'} \frac{\langle E_l | j_\mu | E_{l'} \rangle \langle E_{l'} | j_\nu | E_l \rangle}{E_l - E_{l'}} \times \frac{f(E_{l'} - E_F) - f(E_l - E_F)}{E_l - E_{l'} + \omega - i\alpha} \frac{d^2 k}{(2\pi)^2}, \quad (5)$$

where E_F represents the Fermi energy, $f(E) = 1/(1 + \exp(\beta E))$ the Fermi-Dirac distribution at the inverse temperature β and ω the frequency of the external field. The current operator

$$j_\mu = ie[H, r_\mu] \quad (6)$$

with $r_\mu = i\partial/\partial k_\mu$ has vanishing diagonal elements. First we calculate current matrix elements defined in (5). Due to rotational symmetry of the model, the use of polar coordinates is more convenient. Since the angular variable enters only the current matrix elements, the corresponding integration can be carried out separately. The intraband matrix elements

$$\int_0^{2\pi} \langle \pm E | j_x | \pm E \rangle \langle \pm E | j_y | \pm E \rangle d\varphi = 4e^2 \int_0^{2\pi} n^2 k^{4n-2} \frac{\cos(\varphi) \sin(\varphi)}{4E^2} d\varphi = 0 \quad (7)$$

vanish after angular integration. The nonvanishing inter-band contribution of the matrix elements reads

$$\begin{aligned} & \int_0^{2\pi} \langle \pm E | j_x | \mp E \rangle \langle \mp E | j_y | \pm E \rangle d\varphi = \\ & \pm \int_0^{2\pi} ie^2 n^2 \frac{k^{2n-2}}{E^2} \{mE + ik^{2n} \cos(\varphi) \sin(\varphi)\} d\varphi = \\ & \pm i 2\pi e^2 n^2 k^{2n-2} \frac{m}{E}. \end{aligned} \quad (8)$$

The current matrix elements are imaginary. In order to obtain the real part $\sigma'_{\mu\nu}$ of $\sigma_{\mu\nu}$ we have to evaluate a Cauchy principal value integral

$$\begin{aligned} \sigma'_{\mu\nu} &= \frac{i}{\hbar} \int \sum_{l' \neq l} 2e^2 i\pi n^2 k^{2n-2} \frac{m}{E_l} \frac{1}{E_l - E_{l'}} \\ & \times \frac{f(E_{l'} - E_F) - f(E_l - E_F)}{E_l - E_{l'} + \omega} \frac{k dk}{(2\pi)^2}. \end{aligned} \quad (9)$$

Substituting the k integration by an integration over the energy $E = \sqrt{m^2 + k^{2n}}$, the corresponding Jacobian becomes

$$J = \left(\frac{\partial E}{\partial k} \right)^{-1} = \frac{E}{nk^{2n-1}}. \quad (10)$$

All powers of k in the integrand cancel each other, such that the real part of the Hall conductivity reduces to the simple expression

$$\sigma'_{xy} = \frac{ne^2 m}{\pi \hbar} \int_{|m|}^{\infty} \frac{f(-E - E_F) - f(E - E_F)}{4E^2 - \omega^2} dE. \quad (11)$$

The imaginary part is given by

$$\begin{aligned} \sigma''_{xy} &= \frac{ne^2 m}{\pi \hbar} \int_{|m|}^{\infty} \frac{f(-E - E_F) - f(E - E_F)}{2E} \\ & \times [\delta(2E + \omega) - \delta(2E - \omega)] dE. \end{aligned} \quad (12)$$

In the limits $T \rightarrow 0$ and $E_F \rightarrow 0$ we obtain [6]

$$\sigma'_{xy} = \frac{n}{2} \frac{e^2}{\hbar} \frac{m}{\omega} \ln \left| \frac{2m + \omega}{2m - \omega} \right|, \quad (13)$$

$$\sigma''_{xy} = -\frac{ne^2}{\hbar} \frac{m}{\omega} \theta(\omega - 2m). \quad (14)$$

For $n = 1$ and $n = 2$ this result was also found independently by other authors [21,22,23] and reduces in the DC limit $\omega \rightarrow 0$ to

$$\sigma'_{xy} = \text{sgn}(m) \frac{n}{2} \frac{e^2}{\hbar}, \quad \sigma''_{xy} = 0. \quad (15)$$

This DC result was also found for $n = 1$ [24,25]. Hence, the DC Hall conductivity is a nonzero constant, in units of e^2/\hbar , which is proportional to the spectral exponent n .

The real part of the optical Hall conductivity increases with ω for $\omega < 2m$ and decays like ω^{-1} for large ω . Remarkable is the singularity of σ'_{xy} at $\omega = 2m$ in Eq. (13). It appears when the external frequency ω is equal to the gap

of the electronic system and was also discussed in the context of a band transition [6, 26]. This point of the frequency spectrum separates two different regimes of the two-band model: For $\omega > 2m$ the electronic system can absorb a photon from the external field and create a particle-hole pair, whereas this effect is forbidden for $\omega < 2m$. The real part of the longitudinal conductivity undergoes a jump at $\omega = 2m$ from $\sigma'_{xx} = 0$ if $\omega < 2m$ to $\sigma'_{xx} \approx e^2/h$ if $\omega > 2m$ [6]. The divergent Hall conductivity can be understood as a combined effect of particle-hole creation and an unhindered propagation of the particle-hole pairs. This propagation is given by the electronic two-particle Green's function $(H - \omega/2 + i\epsilon)^{-1}(H + \omega/2 - i\epsilon)^{-1}$ [27], which has an exponential decay for $\omega < 2m$, a power law decay at $\omega = 2m$ and an oscillating behavior for $\omega > 2m$. The singularity of the optical Hall conductivity could be used to determine the gap experimentally either by light [28] or synchrotron radiation [29].

3.1 Finite temperatures

In figure 1 we show a plot of expression (11) as a function of ω and different temperatures. The Hall conductivity scales with n . This is in agreement with QHE experiments, where the plateau of BLG around zero carrier density is two times larger than in MLG [1, 7] and for trilayer graphene three times larger than in MLG [10]. The temperature dependence is controlled by the energy scales of the system. In graphene, a relevant energy scale is either the hopping parameter $t \approx 2.8\text{eV}$ or the gap with a similar energy, which corresponds to a temperature $\approx 32.5 \times 10^3 K$. Therefore, expression (11) is insensitive over a wide range of temperatures $T \ll T_F$, as shown in figure 1. In particular, the gap singularity of the optical Hall conductivity survives. For very high temperatures, however, the Hall conductivity is reduced and goes eventually to zero. This is shown for fixed frequency ω in figure 2.

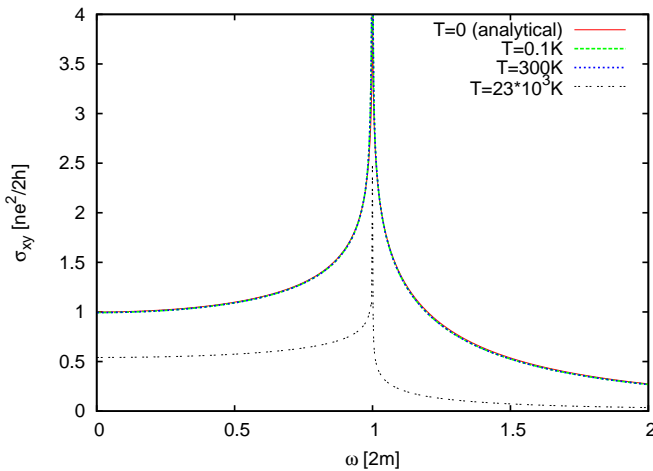


Fig. 1. Frequency and temperature dependence of the optical Hall conductivity.

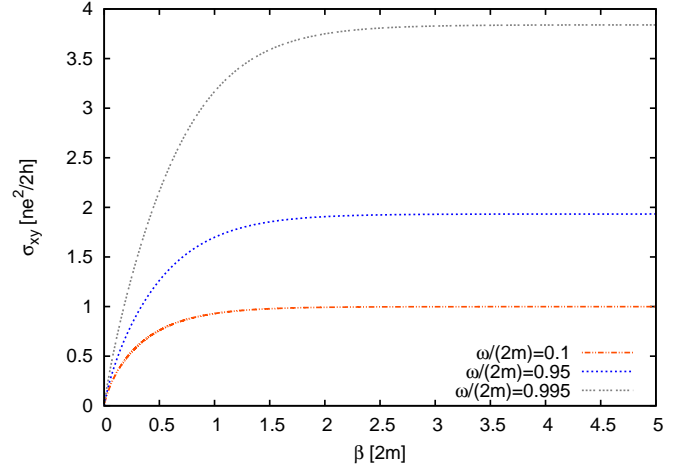


Fig. 2. Optical Hall conductivity near the singularity as a function of the inverse temperature β .

3.2 Disorder

We have seen that thermal fluctuations have almost no effect on the singularity at $\omega = 2m$. Since graphene is also subject to disorder effects (ripples, impurities, etc.), we study their influence on the singularity in the following. Complementary to [16], where the Hall conductivity of Dirac fermions in a random vector potential is calculated numerically, disorder is introduced here via a scattering rate within the self-consistent Born approximation. This is a good approximation for one-particle properties such as the density of states, it fails for the DC ($\omega \rightarrow 0$) conductivity though due to singularities at $\omega = 0$ [30]. However, it is reliable again for the optical conductivity if $\omega \gg \eta$ because the frequency plays the role of a cut-off for the singularities. The latter is also the reason that the optical conductivity is not very sensitive to the type of disorder (e.g., scalar potential, vector potential or gap fluctuations) and the details of the scattering type (e.g., intra- and inter-valley scattering). Thus returning to the Kubo formula (5), we can rewrite the conductivity as (cf. [27])

$$\sigma_{\mu\nu} = \lim_{\alpha \rightarrow 0} \frac{i}{\hbar} \int \int \frac{\langle Tr [j_\mu \delta(H_{dis} - \epsilon') j_\nu \delta(H_{dis} - \epsilon)] \rangle}{\epsilon - \epsilon' + \omega - i\alpha} \times \frac{f_\beta(\epsilon' - E_F) - f_\beta(\epsilon - E_F)}{\epsilon - \epsilon'} d\epsilon d\epsilon', \quad (16)$$

where $\langle \dots \rangle$ represents the disorder average. The latter can be approximated in the self-consistent Born approximation by replacing the Hamiltonian H_{dis} by $\langle H_{dis} \rangle + i\eta$ [5]. The average Hamiltonian $\langle H_{dis} \rangle$ is the same as the Hamiltonian in (2) and η is the scattering rate caused by the disorder. This implies that we have to replace the Dirac delta functions in (16) as

$$\delta(H_{dis} - \epsilon) \rightarrow \delta_\eta(H - \epsilon) = \frac{i}{2\pi} [(H - \epsilon + i\eta)^{-1} - (H - \epsilon - i\eta)^{-1}]. \quad (17)$$

In MLG the scattering rate is $\eta \propto \exp(-\pi/g)$ [31], where g is the variance of the random gap. In BLG, on the other

hand, η is proportional to the variance g , which implies that the influence of disorder on BLG is much stronger. This difference is a consequence of the finite (divergent) density of states at the band edges of MLG (BLG). Realistic fluctuations in graphene near the Dirac node are less than a tenth of the hopping rate $g \approx 0.1$, which can be obtained by extrapolating the measured data obtained away from the Dirac node [32]. This results in scattering rates $\eta \approx 2 \times 10^{-14}$ (MLG) and $\eta \approx 0.1$ (BLG).

Now the trace in Eq. (16) can be expressed again in diagonal representation as

$$\begin{aligned} \text{Tr} [j_\mu \delta_\eta (H - \epsilon') j_\nu \delta_\eta (H - \epsilon)] = \\ \int \langle E_l | j_\mu | E_{l'} \rangle \langle E_{l'} | j_\nu | E_l \rangle \\ \delta_\eta (E_l - \epsilon') \delta_\eta (E_{l'} - \epsilon) \frac{k dk}{(2\pi)^2}. \end{aligned} \quad (18)$$

After angular integration (cf. (8)) and transforming the k -integral to an energy integral the conductivity reads

$$\begin{aligned} \sigma'_{xy} = \frac{e^2 n m}{2\pi \hbar} \int_{|m|=-\infty}^{\infty} \int_{-\infty}^{\infty} \int_{-\infty}^{\infty} \frac{f_\beta(\epsilon' - E_F) - f_\beta(\epsilon - E_F)}{(\epsilon - \epsilon')(\epsilon - \epsilon' + \omega)} \\ \times [\delta_\eta(E - \epsilon') \delta_\eta(-E - \epsilon) - \delta_\eta(-E - \epsilon') \delta_\eta(E - \epsilon)] \\ \times d\epsilon d\epsilon' dE. \end{aligned} \quad (19)$$

We evaluated expression (19) for $T = 0$ and $\mu = 0$ numerically for several values of η . The results are depicted for the real and imaginary part of the optical Hall conductivity in figures 3 and 4. One can see that the Hall plateaux remains nearly constant for all η under consideration, whereas the singularity is broadened.

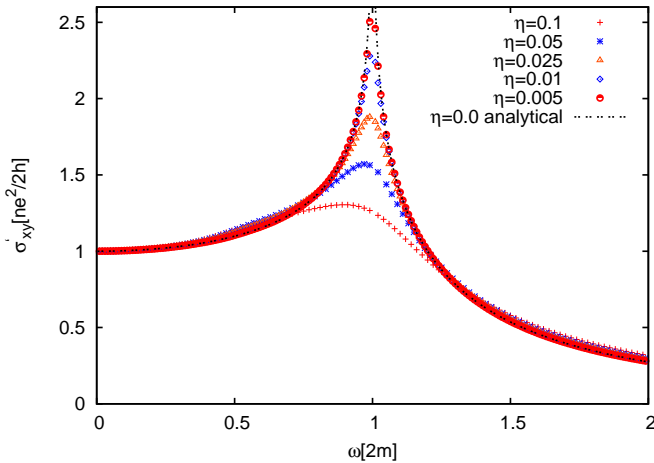


Fig. 3. Real part of the optical Hall conductivity for different values of the scattering rate η .

4 Conclusion

In this work we have studied the optical Hall conductivity for systems with gapped nodes of order n . Our calculations

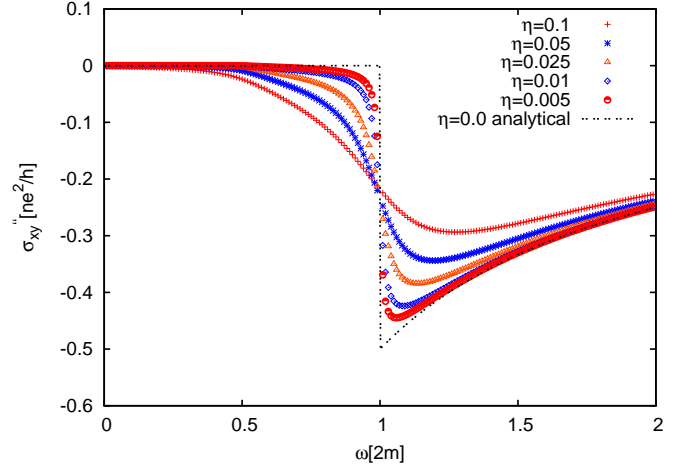


Fig. 4. Imaginary part of the optical Hall conductivity for different values of the scattering rate η .

indicate that the DC Hall conductivity for $n = 1$ and for $n = 2$ only depends on the sign of the mass term and on the exponent of the low-energy spectrum. It reproduces the experimentally observed factor of 2 for BLG. Interesting is that the optical Hall conductivity is quite insensitive to thermal fluctuations over a wide range of temperatures. The effect of the curvature of the low-energy spectrum is also surprisingly simple: The optical Hall conductivity is only multiplied by the factor n , as it was also found for $n = 1, 2$ in case of the longitudinal optical conductivity. It also reflects the n dependence of the visual transparency of multilayer graphene [28]. Interestingly, there is a logarithmic singularity in the optical Hall conductivity when the frequency ω of the external AC field becomes equal to the gap of the electronic system. The appearance of the singularity in our calculations is related to the onset of particle-hole excitations for $\omega \geq 2m$. Although thermal fluctuations have no effect on this singularity, disorder may soften it in the case of $n > 1$, where the scattering rate η can be large. In $n = 1$ case, where the scattering rate is very small, the singularity of the optical Hall conductivity is almost unaffected. Consequently, the singularity could be used to determine the gap in MLG or topological insulators by measuring the optical Hall conductivity.

References

1. K.S. Novoselov, E. McCann, S.V. Morozov, V.I. Fal'ko, M.I. Katsnelson, U. Zeitler, D. Jiang, F. Schedin, A.K. Geim, *Nat. Phys.* **2**, 177 (2006)
2. T. Ohta, A. Bostwick, T. Seyller, K. Horn, E. Rotenberg, *Science* **313**, 951 (2006)
3. J. Cserti, *Phys. Rev. B* **75**, 033405 (2007)
4. E.J. Nicol, J.P. Carbotte, *Phys. Rev. B* **77**, 155409 (2008)
5. D.S.L. Abergel, V. Apalkov, J. Berashevich, K. Ziegler, T. Chakraborty, *Adv. Phys.* **59**, 261 (2010)
6. A. Hill, A. Sinner, K. Ziegler, *New J. Phys.* **13**, 035023 (2011)

7. K.S. Novoselov, A.K. Geim, S.V. Morozov, D. Jiang, Y. Zhang, S.V. Dubonos, I.V. Grigorieva, A.A. Firsov, *Science* **306**, 666 (2004)
8. Y. Zhang, Y. Tan, H.L. Stormer, P. Kim, *Nature* **438**, 201 (2005)
9. N. Nagaosa, J. Sinova, S. Onoda, A.H. MacDonald, N.P. Ong, *Rev. Mod. Phys.* **82**, 1539 (2010)
10. L. Zhang, Y. Zhang, J. Camacho, M. Khodas, I. Zaliznyak, *Nat. Phys.* **7**, 953 (2011)
11. D.C. Elias, R.R. Nair, T.M.G. Mohiuddin, S.V. Morozov, P. Blake, M.P. Halsall, A.C. Ferrari, D.W. Boukhvalov, M.I. Katsnelson, A.K. Geim, K.S. Novoselov, *Science* **323**, 610 (2009)
12. T. Morimoto, Y. Hatsugai, H. Aoki, *Phys. Rev. Lett.* **103**, 116803 (2009)
13. V.P. Gusynin, S.G. Sharapov, *Phys. Rev. B* **73**, 245411 (2006)
14. V.P. Gusynin, S.G. Sharapov, J.P. Carbotte, *J. Phys.: Condens. Matter* **19**, 026222 (2007)
15. F.D.M. Haldane, *Phys. Rev. Lett.* **61**, 2015 (1988)
16. K. Nomura, N. Nagaosa, *Phys. Rev. Lett.* **106**, 166802 (2011)
17. A.H. Castro Neto, F. Guinea, N.M.R. Peres, K.S. Novoselov, A. Geim, *Rev. Mod. Phys.* **81**, 109 (2009)
18. E. McCann, V.I. Fal'ko, *Phys. Rev. Lett.* **96**, 086805 (2006)
19. H. Min, A.H. MacDonald, *Phys. Rev. B* **77**, 155416 (2008)
20. F. Zhang, B. Sahu, H. Min, A.H. MacDonald, *Phys. Rev. B* **82**, 035409 (2010)
21. W.-K. Tse, A.H. MacDonald, *Phys. Rev. Lett.* **105**, 057401 (2010)
22. R. Nandkishore, L. Levitov, *Phys. Scr.* **T146**, 014011 (2012)
23. E.V. Gorbar, V.P. Gusynin, A.B. Kuzmenko, S.G. Sharapov, *Phys. Rev. B* **86**, 075414 (2012)
24. G.W. Semenoff, *Phys. Rev. Lett.* **53**, 2449 (1984)
25. N.A. Sinitsyn, J.E. Hill, H. Min, J. Sinova, A.H. MacDonald, *Phys. Rev. Lett.* **97**, 106804 (2006)
26. R. Nandkishore, L. Levitov, *Phys. Rev. Lett.* **107**, 097402 (2011)
27. K. Ziegler, *Phys. Rev. B* **75**, 233407 (2007)
28. R.R. Nair, P. Blake, A.N. Grigorenko, K.S. Novoselov, T.J. Booth, T. Stauber, N.M.R. Peres, A.K. Geim, *Science* **320**, 1308 (2008)
29. Z.Q. Li, E.A. Henriksen, Z. Jiang, Z. Hao, M.C. Martin, P. Kim, H.L. Stormer, D.N. Basov, *Nat. Phys.* **4**, 532 (2008)
30. K. Ziegler, *Physica E* **40**, 2622 (2008)
31. K. Ziegler, *Phys. Rev. B* **79**, 195424 (2009)
32. Y.-W. Tan, Y. Zhang, K. Bolotin, Y. Zhao, S. Adam, E. Hwang, S. Das Sarma, H. L. Stormer, and P. Kim, *Phys. Rev. Lett.* **99**, 246803 (2007)